Open Access Journal

Journal of Power Technologies 97 (4) (2017) 370–377

journal homepage:papers.itc.pw.edu.pl

Predicting Chemical Flame Lengths and Lift-off Heights in Enclosed, Oxy-Methane Diffusion Flames at Varying O_2/CO_2 Oxidizer Dilution Ratios

Gautham Krishnamoorthy[a,*], Mario Ditaranto[b]

[a] *Department of Chemical Engineering, Harrington Hall Room 323, 241 Centennial Drive, University of North Dakota, Grand Forks, ND 58202-7101, USA;*
[b] *SINTEF Energy Research, 7465 Trondheim, Norway*

Abstract

Experiments have shown reactor confinement, wall temperatures and radiative transfer to influence the flame length and lift-off characteristics of oxy-methane flames. In this study, the performances of the Shear Stress Transport (SST) k-ω turbulence model, a skeletal methane combustion mechanism (16 species and 41 reactions) and two weighted sum of gray gas models (WSGGM) towards capturing these flame characteristics are evaluated against measurements obtained from oxy-methane flames across a wide range of oxidizer O_2/CO_2 ratios and fuel Reynolds numbers. Gas composition, gas and wall temperatures, flame length measurements and inferences of lift-off heights from OH* chemiluminescence imaging are employed in the assessment. The corresponding numerical estimate of flame length and lift-off heights were made by determining the flame shape by the locus of points at which the CO concentrations reduce to 1% of their peak values within the flame.

The predicted gas temperatures and compositions compared reasonably well against measurements. The criterion for defining the flame shape based on CO concentrations appears promising since the trends in chemical flame length and lift-off height predictions agreed reasonably well with the measurements across the range of oxidizer concentrations and fuel Reynolds numbers. Flame length prediction sensitivities to the wall temperatures and the WSGGM model were also assessed.

Keywords: Oxy-methane; combustion model; flame length; lift-off height; WSGGM

1. Introduction

Oxy-combustion technologies for both coal [1] and natural gas [2] fired power plants have been shown to be a promising option for CO_2 capture. It has been estimated that the specific CO_2 emissions from natural gas combined cycle (NGCC) power plants can be reduced from current levels of approximately 350 g CO_2/kWh to far below 100 g CO_2/kWh by employing Carbon Capture with Sequestration technologies [3]. The main approach in oxy-fuel combustion technology is to replace air in the oxidizer stream with a mixture of pure O_2 and a recycled flue gas stream consisting mainly of CO_2. However, due to differences in the thermal and chemical effects associated with replacing N_2 with CO_2, the design of combustors must be adapted [2]. Therefore, oxy-methane combustion scenarios have been investigated experimentally as well as numerically by several researchers [4–6].

Experimental investigations of Kutne et al. [7] showed a strong effect of the O_2 content in the oxidizer on diffusion flame stability. O_2 concentrations of 27–30% by volume in the oxidizer have been deemed to be necessary to achieve stable combustion behavior in oxy-methane flames [7, 8]. However, recent studies have also shown that the wall temperature has a significant effect on the lift-off of methane jet flames in O_2/CO_2 atmospheres with higher wall temperatures appearing to have a stabilizing effect on the flame [9]. The wall temperature profiles are in turn a result of the flame length, gas temperatures, wall incident radiative fluxes and convective heat transfer patterns within the furnace. Further, reactor confinement has been shown to result in longer flames when compared against unconfined oxy-flames [10]. Recent measurements of radiative heat fluxes from oxy-methane flames in confined reactors also show an increase in radiative intensities with oxygen enrichment in oxy-combustion scenarios [11]. Therefore, accurate modeling of the gas-phase chemistry, turbulence and radiative heat transfer are necessary to understand the stability, flame length and lift-off characteristics of oxy-flames.

Previous computational fluid dynamic (CFD) studies have augmented our understanding of oxy-methane combustion behavior and led to the identification of combustion mod-

*Corresponding author
Email address: gautham.krishnamoorthy@engr.und.edu (Gautham Krishnamoorthy)

els that have been deemed to be appropriate for simulating these scenarios. However, most of the validations were of unenclosed flames [12] or semi-industrial scale systems exhibiting a strong interplay between turbulence and chemistry [13]. Due to the practical significance of enclosed reactors the goal of this study is to provide an initial assessment of turbulence, detailed chemistry and radiative property models towards capturing the flame height and lift-off characteristics through comparisons against high-fidelity experimental data-sets obtained in an enclosed reactor for a wide range of oxidizer O_2/CO_2 ratios. Particular emphasis is placed on ensuring the availability of wall temperature measurements that can be enforced as thermal boundary conditions in the simulations with the goal of minimizing their impact on the chemical flame lengths and lift-off height predictions.

Obtaining numerical estimates of the flame length and lift-off heights is challenging due to: the fact that there are at least seven different ways in which they can be defined [14], predictions in small flames are sensitive to the wall temperatures and thermal boundary conditions employed in the simulations, and predictions are also sensitive to the turbulence boundary conditions employed at the fuel and co-flow inlets [15, 16].

These challenges are addressed in the following manner: Recent studies appear to suggest that defining the flame shape by the locus of points at which the CO concentrations reduce to 1% of its peak values within the flame, appears to give the best agreement with experimental measurements [14, 17, 18]. Therefore, one of the goals of this study was to examine the validity of estimating the chemical flame length and lift-off heights by defining the flame shape in this manner for a wide range of O_2/CO_2 ratios in the oxidizer stream and fuel jet Reynolds numbers (Re 2340–10776). Second, the measured wall temperature measurements are fit to a profile and enforced as thermal boundary conditions in the simulations.

High-fidelity measurements from enclosed flames for a wide range of oxidizer O_2/CO_2 ratios were employed to assess the performances of the combustion models. Experimental measurements of temperature and gas composition from confined, transitional (Re 2340), methane flames in oxidizer compositions of: 21% O_2 – 79% N_2, 35% O_2 – 65% CO_2, 50% O_2 – 50% CO_2 and 70% O_2 – 30% CO_2 are first reported in this study. Gas composition, flame length, gas and wall temperature measurements are then employed to assess the performances of: the Shear Stress Transport (SST) k-ω turbulence model, and a skeletal mechanism (16 species and 41 reactions). The SST k-ω turbulence model with Low-Re-number correction was employed in the simulations since we found that it was able to resolve the turbulence well in the buoyant regions outside the flames at the lower elevations within the furnace. The gas-phase radiative properties of H_2O and CO_2 were estimated employing two weighted sum of gray gas models (WSGGM) that have both been previously validated for oxy-combustion scenarios [19, 20]. However, a recent study encompassing four different WSGGM showed that while the radiation predictions between these two models are generally within 25–30% at high temperatures (> 800 K), the differences can be as much as 95% in the temperature region 500 K–800 K, due to differences in the spectroscopic databases employed in their formulation and the accuracies of the curve-fitting procedure [21]. In most industrial applications, radiation is dominated by the high temperature gases and these differences may not have a significant impact on the gas temperature and wall radiative flux predictions [22, 23]. However, since the oxy-flames investigated in this study have significant oxygen enrichment in the oxidizer stream (up to 70%) the resulting temperatures are higher than conventional combustion scenarios. Further, due to the high concentrations of the radiatively participating gases, we anticipate even these modest differences in the WSGGM predictions to have an impact on the flame-length and lift-off predictions by influencing the temperature predictions. Both the WSGGM were therefore implemented in this study as User-Defined Functions (UDFs) and employed in conjunction with the CFD code ANSYS FLUENT® [24]. Unless otherwise mentioned, the WSGGM from Krishnamoorthy [19] was employed as the primary modeling option in this study.

2. Theory

2.1. Experimental Conditions

Fig. 1a provides the geometric details of the furnace investigated in this study.

The furnace consists of a cylindrical geometry with a fuel nozzle of diameter 5 mm and an oxidizer nozzle of diameter 100 mm. These were enclosed in a stainless steel walled combustion chamber of diameter 350 mm and length 1000 mm. The large dimension of the furnace relative to that of the flame minimized interaction and perturbation of the flow with the wall. The oxidizer gas was sent through a series of perforated plates to ensure uniform velocity distribution. The inside faces of the stainless steel walls of the reactor were coated with a blackbody paint of emissivity 0.98. The temperature and gas concentration (CO, CO_2 and O_2) profiles around the flames were measured at four axial heights and in a radial direction from the wall until the vicinity of the outer limit of the flame as defined as when the CO concentration increased sharply. The wall temperature measurements were made up to 615 mm along the height of the furnace. The measured wall temperatures were then fit to a profile and imposed as thermal boundary conditions as shown in Fig. 1b. Since the flow conditions inside the reactor resulted in thermal stratification of the gases outside the flame due to buoyancy, the two axial measurement locations near the bottom of the reactor were at stagnant zones, where the velocities and turbulent kinetic energy production were anticipated to be small. This was confirmed through the strong recirculation patterns that were observed experimentally via a decrease in gas temperature close to the walls as a result of downward flow. The top two axial locations were located right below the tip of the flames and above the flames

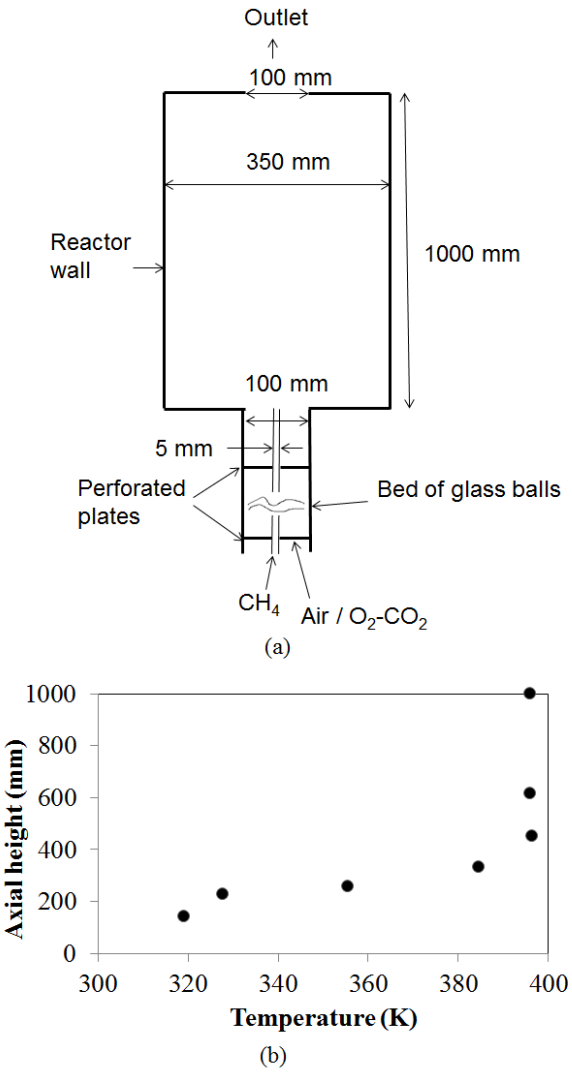

Figure 1: (a) Geometric details of the furnace; (b) Wall temperature (K) employed as thermal boundary condition along the axial direction

respectively. Since the flame lengths vary with the O_2/CO_2 oxidizer dilution ratios, the choice of the axial measurement locations also varied among the flames.

The gas was sampled with a quartz probe and analyzed with conventional gas analyzers and the temperature profiles were obtained by transversing radially, four equally spaced 500 μm fine bead thermocouples in the gas layer. Obtaining reliable species profiles within these small laboratory flames requires non-intrusive laser diagnostics, which were not applied in this study. The usage of the sampling probe was therefore limited to regions where its measurements could be trusted. The co-flow velocity and fuel velocity were maintained at 0.25 m/s and 7.6 m/s, respectively. The inlet temperature of the fuel was maintained at 288 K for the fuel densities to match the fuel inlet Reynolds number of 2340. The measurements were repeated three times on different days with different experimental operating histories. The average

Table 1: A summary of methane flames investigated in this study

Fuel jet Reynolds number	Oxidizer compositions	Variables measured
2340	21% O_2–79% N_2, 35% O_2–65% CO_2, 50% O_2–50% CO_2, 70% O_2–30% CO_2	Gas temperature, compositions, flame lengths, wall temperatures
4618–10776	35% O_2–65% CO_2, 50% O_2–50% CO_2	Wall temperatures, lift-off heights

Table 2: Summary of physical models employed in the CFD simulations

Physical Models	Modeling option
Gas-Phase chemistry	EDC with a 41-step skeletal mechanism (Smooke [25])
Gas-Phase radiative property	Perry (5 gg) [19]* (primary modeling option), EM2C (5 gg) [20]* (secondary modeling option)
Turbulence	SST k-ω [24]
Radiative transport equation solver	Discrete ordinates method (Angular resolution, theta x phi: 3 x 3) [24]

*These models were implemented as User-Defined Functions (UDFs) in ANSYS FLUENT

of the three measurements is reported in this study. The measurement variations were found to be within the range of measurement uncertainties.

The lift-off measurements were carried out in the same geometry at oxygen concentrations ranging from 34–50% and a co-flow velocity of 0.4 m/s. Experimental inferences of lift-off height were made by averaging narrow band filtered images of OH* chemiluminescence (308 nm +/- 5 nm) with an intensified CCD camera [9]. An average of more than 100 instantaneous images was calculated and a threshold intensity defined as half of the maximum average intensity was used to determine the lift-off height. In addition, the furnace wall temperatures were carefully measured during the experiment. In the lift off study, the wall temperatures were seen to vary from the range shown in Fig. 1b for small flames to around 650 K for the large (high fuel velocity) flames. However, for comparison against numerical predictions reported in this study, we have ensured consistency between the measured wall temperatures and those imposed as thermal boundary conditions at the walls.

Therefore, in addition to the Re 2340 flames mentioned previously, additional simulations were carried out at co-flow velocities of 0.4 m/s, and fuel inlet Reynolds numbers in the range 4618–10776 and compared against those measurements reported in [9]. The flames investigated in this study are summarized in Table 1.

2.2. CFD Modeling Approach

The CFD simulations were carried out using the commercial code ANSYS FLUENT [24] with user-defined add-on models [19, 20] for accurately predicting the radiative properties of gases and to compute the flame radiation to the wall and CO_2 re-absorption. The furnace was modeled in a 2D axisymmetric domain to take advantage of the symmetry of the problem. The geometry was meshed employing 31,246 hexahedral control volumes. The meshes near the wall was

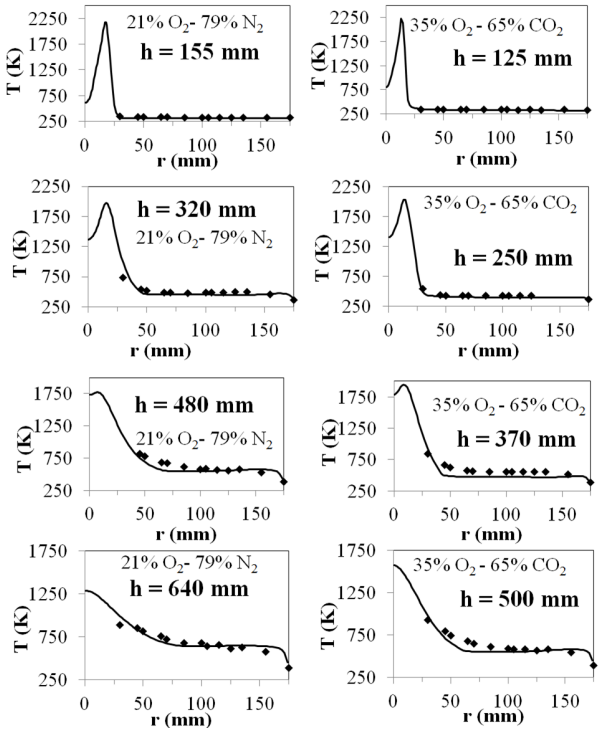

Figure 2: Radial temperature profiles in: 21% O_2–79% N_2 flame (left); 35% O_2–65% CO_2 flame (right) (—SST k-ω; ♦ measurements)

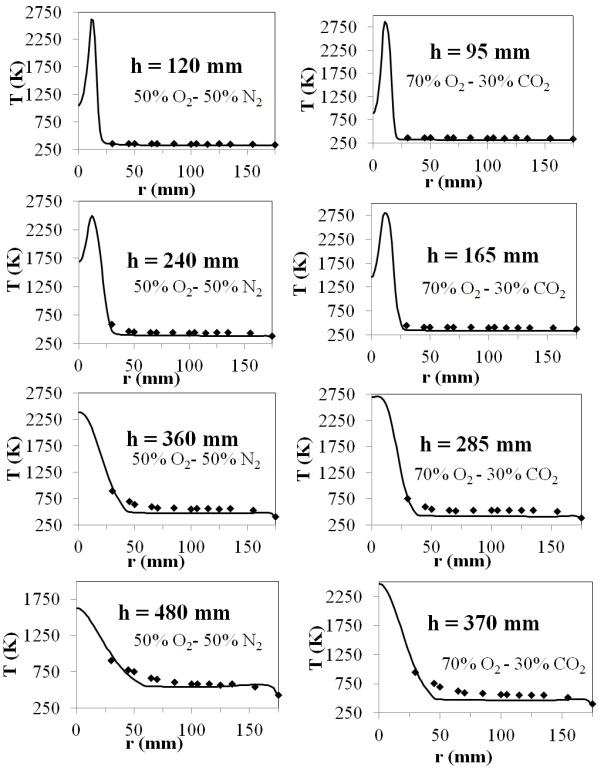

Figure 3: Radial temperature profiles in: 50% O_2–50% CO_2 flame (left); 70% O_2–30% CO_2 flame (right) (—SST k-ω; ♦ measurements)

made fine enough to adequately resolve the viscous sublayer (y+ $\sim$ 1). Further refinement of the mesh did not change the results reported here. The pressure-velocity coupling was accomplished using the SIMPLEC algorithm [26] which we have determined from past experience to perform well in such buoyancy driven enclosure flows where the laminar Froude numbers were less than unity [11]. The PRESTO [27] and QUICK [28] schemes were employed for the spatial discretization of the pressure, momentum, turbulence and species equations since hexahedral cells were employed in the calculations. The boundary conditions for the turbulence model at the flow inlets were assigned a turbulence intensity of 5% along with the hydraulic diameter (5 mm for the fuel inlet and 100 mm for the oxidizer inlet respectively). Changes to the turbulence intensities as will be reported later in this study did not change the flame lengths reported in this study by more than 2.5%. For boundary conditions for the radiation model, the stainless steel walls of the furnace were assigned an emissivity of 0.98 at the inside walls of the reactor and the temperature measurements reported in Fig. 1b were implemented as a profile function. The different CFD modeling options adopted in this study are summarized in Table 2.

3. Results and Discussion

3.1. Temperature

Figures 2 and 3 compare the numerical temperature predictions against experimental measurements along the radial direction at different axial locations for both air and oxy- combustion flames. The axial centerline ($r = 0$) corresponds to the flame center. Predictions from the SST k-ω and skeletal 41-step chemistry models are in reasonable agreement with the measurements. Since the highest axial measurement locations were just beyond the flame lengths, a decrease in flame length with an increase in O_2 concentrations in the oxidizer stream is seen. The stoichiometric mixture fraction increases with an increase in oxidizer O_2 concentration, which displaces the flame front to lower axial locations.

Further, an increase in centerline temperature with an increase in oxidizer O_2 concentrations is also observed due to a decrease in the heat that is absorbed by CO_2.

3.2. O_2

Figures 4 and 5 compare the numerical variations in O_2 concentrations (mol % dry basis) against experimental measurement along the radial direction for both air and oxy-fuel combustion cases. A reasonably good agreement is again obtained between the numerical predictions and the measurements.

3.3. Flame length

Numerical estimates of the chemical flame length were made by estimating the flame shape by the locus of points where the CO mole fractions reduced to 1% of their peak value i.e., $R_{CO} = Y_{CO}/Y_{CO,max} = 0.01$ [14]. The chemical flame

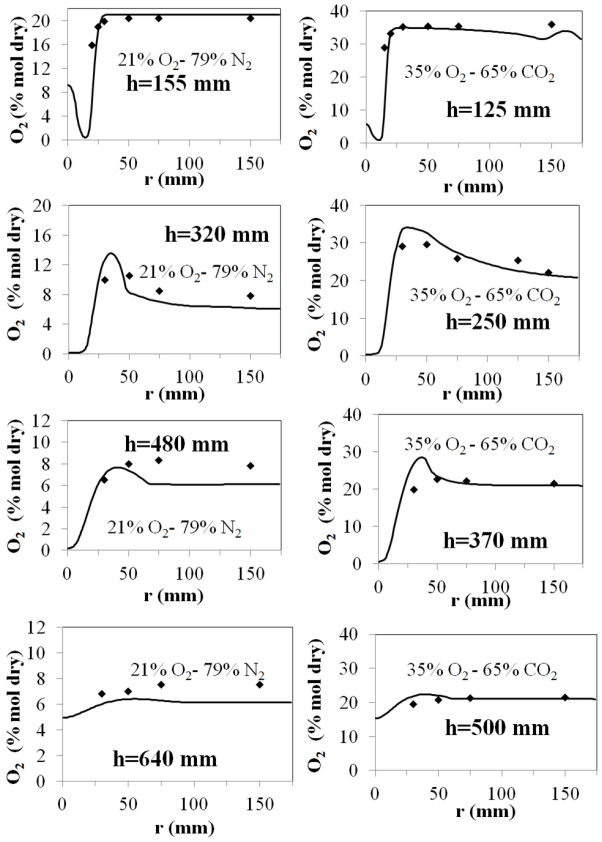

Figure 4: Radial O_2 profiles in: 21% O_2–79% N_2 flame (left); 35% O_2–65% CO_2 flame (right) (—SST k-ω; ♦ measurements)

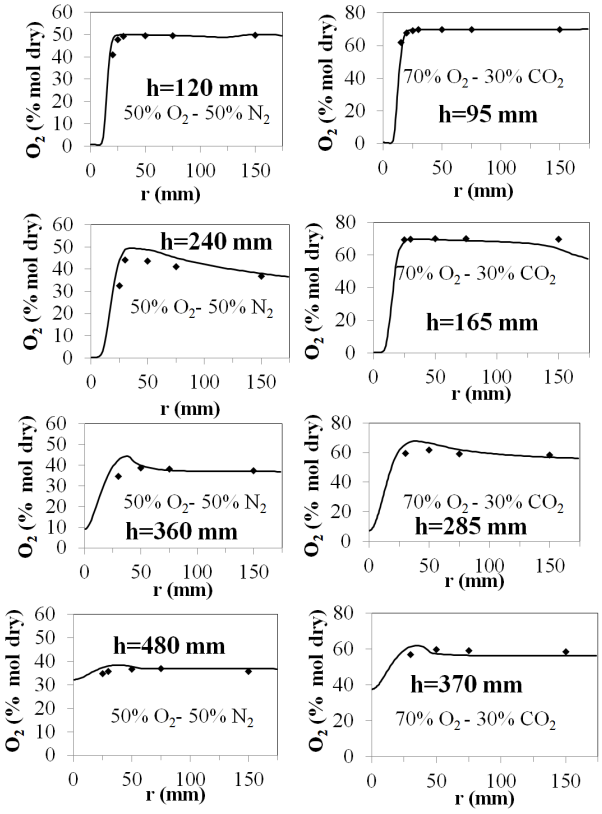

Figure 5: Radial O_2 profiles in: 50% O_2–50% CO_2 flame (left); 70% O_2–30% CO_2 flame (right) (—SST k-ω; ♦ measurements)

length predictions are compared against experimental measurements in Fig. 6. Consistent with experimental observations, the models predict a decrease in flame length with an increase in O_2 concentration in the oxidizer stream with the agreement with experimental data improving at higher oxidizer concentrations. To ascertain this, an additional simulation was carried out with 100% O_2 in the oxidizer stream. This resulted in a flame length of 400 mm, which agrees very well with the flame length measurements of pure O_2 fired oxy-flames reported by Kim et al. [29] at similar Reynolds numbers. In order to investigate the sensitive of the flame length predictions to the turbulence boundary conditions, the turbulence intensities at the fuel inlet was varied from 1% to 10% corresponding to a two-order of magnitude variation in the turbulent kinetic energy of the fuel (from 0.00866 m^2/s^2 to 0.866 m^2/s^2). However, the flame length variations was less than 2.5% between these two extremes for all the flames that were investigated.

3.4. Lift-off Height

Previous investigations of lift-off height variations in oxy-methane flames have determined that with an increase in O_2 concentrations in the oxidizer stream the lift-off heights in the flames are reduced [9]. Further, the lift-off heights were found to be strongly sensitive to the wall temperature. In this study, numerical estimates of the lift-off height were made from the estimated flame shapes by the locus of points where the CO mole fractions reduced to 1% of their peak value i.e., $R_{CO} = Y_{CO}/Y_{CO,max} = 0.01$ and compared against the experiments.

The lift-off height measurements were made in the same reactor geometry at higher fuel Reynolds numbers (cf. Table 1). However, the co-flow velocity in the experiments was maintained at 0.4 m/s and a range of fuel inlet velocities and oxidizer compositions were investigated. Experimental inferences of lift-off height were made by averaging narrow band filtered images of OH* chemiluminescence (308 nm +/- 5 nm) with an intensified CCD camera. Therefore, numerical simulations of selected flames from the lift-off study [9] were carried out employing the SST k-ω model and co-flow velocity of 0.4 m/s. Figure 7 compares the predicted lift-off results against the numerical estimates for fuel inlet velocities of 15 m/s (Re 4618) to 35 m/s (Re 10776) and oxidizer compositions of 35% O_2/65% CO_2 and 50% O_2/50% CO_2. The temperature profile shown in Fig. 1b was maintained as the reactor wall temperature. While comparing the numerical simulations against the experimental measurements, we have ensured that the comparisons were made against data where the measured reactor wall temperatures were identical/in the range of the wall thermal boundary conditions enforced in the simulations. A very good agreement is seen between the simulations and the predictions in Fig. 7. Further, the simulations were able to correctly predict a decrease in

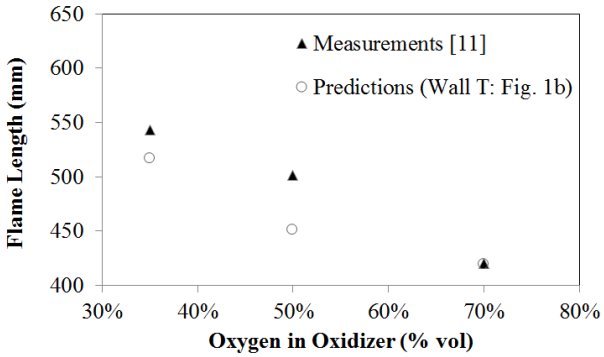

Figure 6: Chemical Flame length predictions for the three (Re 2340) oxy-flames examined in this study

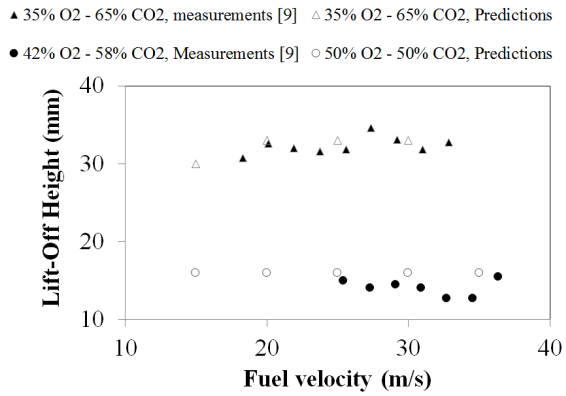

Figure 7: Lift-off height predictions and measurements at different oxidizer compositions

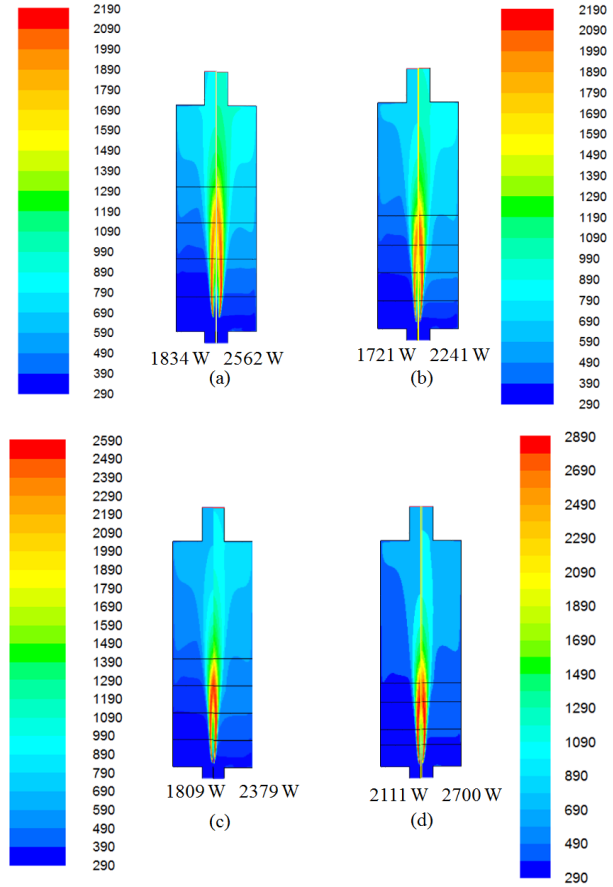

Figure 8: Effect of wall boundary conditions on the temperature contours for the four (Re 2340) flames examined in this study. Oxidizer is: (a) Air; (b) 35% O_2–65% CO_2; (c) 50% O_2–50% CO_2; (d) 70% O_2–30% CO_2. (Left: Wall temperature profile from Fig. 1b; Right: Fixed wall temperature of 600 K). Total radiative fluxes are also indicated at the bottom

lift off height with an increase in O_2 concentrations in the oxidizer stream.

3.5. Effect of wall temperature

In order to further quantify the effect of the wall temperature on the flame length, additional simulations of the three Re 2340 oxy-flames were carried out employing a fixed wall temperature of 600 K. The gas temperature contours within each flame are shown in Fig. 8. The left half of each flame corresponds to results from imposing a wall temperature profile shown in Fig. 1b and the right half correspond to a fixed wall temperature of 600 K. The total radiative fluxes within the reactor are also indicated at the bottom of the contours. The impact of imposing the higher wall temperatures on the flame lengths is shown in Fig. 9. Higher wall temperatures increase the flame lengths by increasing the gas temperatures through thermal radiative feedback.

However, simulations of the high Reynolds number flames discussed earlier showed the lift-off heights to be invariant with the higher wall temperatures. Experimentally, the sensitivity of lift-off heights to the wall temperature were clearly observed at fuel velocities over 25 m/s [9]. However, during the experiments the increase in fuel velocity also resulted in longer flames which caused rapid heating of the reactor walls by convection and radiation causing significant wall temperature variations within minutes [9]. This increased uncertainty associated with the wall temperatures might have contributed to the discrepancy between the experimental observations and numerical predictions in terms of the lift-off prediction sensitivities to the thermal boundary conditions and needs to be investigated further.

3.6. Effect of WSGGM

While all of the WSGG models employed in this study have been validated through comparisons against benchmark/line-by-line (LBL) data for prototypical problems [19, 20] in the general temperature range 1000 K–2000 K, a previous study demonstrated that differences in the spectroscopic/model databases employed in the WSGGM formulations resulted in more than a 60% variation in the volume integrated radiative source term predictions in oxy-flames [21]. The total power of the Re 2340 flames investigated in this study was 5 kW (based on the heating value and flow rate of methane). Fig. 8 shows that depending on the wall temperatures approximately 35–50% of the total power is lost as radiation. In a previous

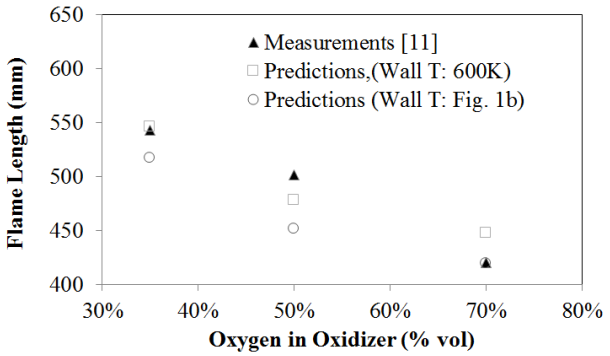

Figure 9: Effect of wall temperature on Chemical Flame length for the three (Re 2340) oxy-flames examined in this study

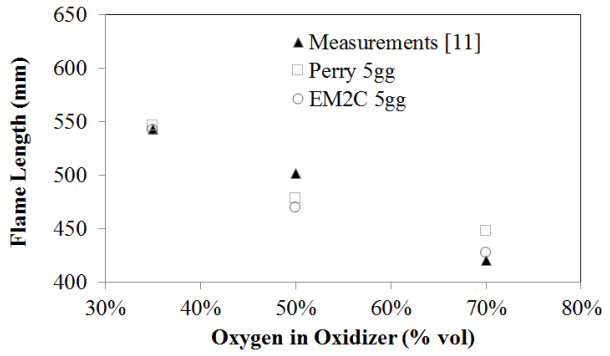

Figure 10: Effect of WSGGM on Chemical Flame length predictions for the three (Re 2340) oxy-flames examined in this study

study around 60% of the radiation was determined to stem from within the flame with the remaining contribution from the high temperature flue gases surrounding the flame [21]. Since radiative transfer impacts the temperature field through the radiative source term in the energy equation, a 25% variation in the radiative source term in the high temperature regions (> 800 K) among the two WSGGM translates to 5–7.5% (0.35 x 0.6 x 0.25 and 0.5 x 0.6 x 0.25 respectively) differences in the predicted temperature field. At peak temperatures of 2500 K and above encountered in the oxy-flames (cf. Fig. 8) this translates to temperature differences of 125–200 K among the WSGGM which could have a bearing on the flame length predictions. In order to examine this impact, simulations of the Re 2340 flames investigated in this study were carried out employing the EM2C 5 gg radiative property model also [20]. A previous study showed that the radiative source term predictions (which represents emission) from the EM2C (5 gg) model were 25–35% higher than those employing the Perry (5 gg) model in the high temperature regions within the flame [21]. Consequently, simulations confirmed that the temperature predictions employing the EM2C (5 gg) model was lower than those employing the Perry (5 gg) by as much as 60 K in the 35% O_2–65% CO_2 oxy flames and by 190 K in the 70% O_2–30% CO_2 oxy-flames. Fig. 10 examines the impact of these variations on the flame length predictions. At low oxidizer O_2 concentrations, the small differences in temperatures are not significant enough to impact the flame lengths. However, the differences among the WSGGM flame length predictions increases as the temperature increases with the oxidizer O_2 concentrations. The EM2C 5 gg model which predicts lower temperatures than the Perry 5 gg model consequently predicts lower flame lengths as well. Again, the lift-off heights that are determined primarily at low temperatures near the burner were not found to be impacted by the choice of WSGGM as the differences in temperature predictions between the models were minimal in this region.

4. Summary/Conclusions

Previous studies have shown that reactor confinement and wall temperature play an important role in determining the lift-off and flame length characteristics of oxy-methane flames. The goal of this manuscript was to provide an initial assessment of combustion and radiation models that can accurately predict the convective flow patterns and radiative transfer and lead to accurate characterization of lift-off heights and flame lengths in oxy-methane flames across a wide range of oxidizer O_2/CO_2 ratios and fuel Reynolds numbers.

To support and validate the simulations in this study, experimental measurements of gas composition, flame lengths, gas and wall temperatures from four enclosed, oxy-methane flames at fuel Reynolds number of 2340 and a wide range of O_2/CO_2 dilution ratios in the oxidizer stream were first reported. This data was supplemented by inferences of lift-off height made from filtered imaging of OH* chemiluminescence at fuel Reynolds numbers in the range 4618–10776. The Shear Stress Transport (SST) k-ω model in conjunction with a skeletal methane combustion mechanism (16 species and 41 reactions) was employed to model the turbulence and chemistry respectively. The gas-phase radiative properties were estimated employing two weighted-sum-of-gray-gas model (WSGGM) formulations with five gray gases implemented as add-on functions. Based on the results from this study the following conclusions may be drawn:

1. The predicted gas temperatures and major gas compositions (O_2) compared reasonably well against the experimental measurements.
2. Numerical estimates of the chemical flame length and lift off height were made by estimating the flame shape by the locus of points where the CO mole fractions reduced to 1% of their peak value i.e., $R_{CO} = Y_{CO}/Y_{CO,max} = 0.01$. A decrease in chemical flame length with an increase in O_2 concentration in the oxidizer was predicted numerically.
3. The lift-off predictions also followed the experimental observations of a decrease in lift-off height with an increase in O_2 concentration in the oxidizer stream. Further, the simulated lift-off heights agreed well against experimental inferences made from filtered imaging of OH* chemiluminescence. Due to the wide range of

flames and oxidizer compositions investigated in this study, the $R_{CO} = Y_{CO}/Y_{CO,max} = 0.01$ criterion recently proposed by Mei et al. [17] appears to be an accurate indicator of the flame shape among the several different definitions of chemical flame lengths in the literature.

4. Simulations also show the role of wall temperature towards influencing the radiation characteristics which impacted flame length predictions. Higher wall temperatures increased the flame lengths. They also caused the radiatively participating gases outside the flames to get hotter thereby enhancing the radiative fluxes at the reactor walls.
5. The predicted flame lengths and flame temperatures were found to be sensitive to the WSGGM employed to compute the radiative properties. Differences in the spectroscopic/model databases employed in the WSGGM formulations resulted in 25–35% differences in the radiative source term predictions between the WSGGM in the high temperature regions within the flame. This translated to 60–190 K variation in the flame temperatures with the differences increasing with an increase in oxidizer O_2 concentrations (and peak flame temperatures). However, at low oxidizer O_2 concentrations, the differences in temperatures were not significant enough to impact the flame lengths.

Acknowledgments

Mario Ditaranto was funded by the BIGCCS Centre, performed under the Norwegian research program Centers for Environment-friendly Energy Research (FME) and acknowledges the following partners for their contributions: ConocoPhillips, Gassco, Shell, Statoil, TOTAL, GDF SUEZ and the Research Council of Norway (193816/S60).

References

[1] R. Soundararajan, T. Gundersen, M. Ditaranto, Oxy-combustion coal based power plants: study of operating pressure, oxygen purity and downstream purification parameters, Chemical Engineering Transactions 39 (2014) 229–234.

[2] S. G. Sundkvist, A. Dahlquist, J. Janczewski, M. Sjödin, M. Bysveen, M. Ditaranto, Ø. Langørgen, M. Seljeskog, M. Siljan, Concept for a combustion system in oxyfuel gas turbine combined cycles, Journal of Engineering for Gas Turbines and Power 136 (10) (2014) 101513.

[3] R. Stanger, T. Wall, R. Spoerl, M. Paneru, S. Grathwohl, M. Weidmann, G. Scheffknecht, D. McDonald, K. Myöhänen, J. Ritvanen, et al., Oxyfuel combustion for CO2 capture in power plants, International Journal of Greenhouse Gas Control 40 (2015) 55–125.

[4] P. Glarborg, L. L. Bentzen, Chemical effects of a high co2 concentration in oxy-fuel combustion of methane, Energy & Fuels 22 (1) (2007) 291–296.

[5] W. Jerzak, The effect of adding co2 to the axis of natural gas combustion flame on the variations in co and nox concentrations in the combustion chamber, Journal of Power Technologies 94 (3) (2014) 202–210.

[6] S. Hjartstam, F. Normann, K. Andersson, F. Johnsson, Oxy-fuel combustion modeling: performance of global reaction mechanisms, Industrial & Engineering Chemistry Research 51 (31) (2012) 10327–10337.

[7] P. Kutne, B. K. Kapadia, W. Meier, M. Aigner, Experimental analysis of the combustion behaviour of oxyfuel flames in a gas turbine model combustor, Proceedings of the Combustion Institute 33 (2) (2011) 3383–3390.

[8] M. Ditaranto, J. Hals, Combustion instabilities in sudden expansion oxy–fuel flames, Combustion and Flame 146 (3) (2006) 493–512.

[9] B. L. Norheim, Lift-off of methane jet flames in o2/co2 atmospheres, Master's thesis, Norwegian University of Science and Technology (2009).

[10] J. Sautet, L. Salentey, M. Ditaranto, J. Samaniego, Length of natural gas-oxygen non-premixed flames, Combustion science and technology 166 (1) (2001) 131–150.

[11] M. Ditaranto, T. Oppelt, Radiative heat flux characteristics of methane flames in oxy-fuel atmospheres, Experimental Thermal and Fluid Science 35 (7) (2011) 1343–1350.

[12] K. Bhadraiah, V. Raghavan, Numerical simulation of laminar co-flow methane–oxygen diffusion flames: effect of chemical kinetic mechanisms, Combustion Theory and Modelling 15 (1) (2010) 23–46.

[13] C. Galletti, G. Coraggio, L. Tognotti, Numerical investigation of oxy-natural-gas combustion in a semi-industrial furnace: validation of cfd sub-models, Fuel 109 (2013) 445–460.

[14] Z. Mei, J. Mi, F. Wang, P. Li, J. Zhang, Chemical flame length of a methane jet into oxidant stream, Flow, Turbulence and Combustion 4 (94) (2015) 767–794.

[15] F. Christo, B. B. Dally, Modeling turbulent reacting jets issuing into a hot and diluted coflow, Combustion and flame 142 (1) (2005) 117–129.

[16] A. Frassoldati, P. Sharma, A. Cuoci, T. Faravelli, E. Ranzi, Kinetic and fluid dynamics modeling of methane/hydrogen jet flames in diluted coflow, Applied Thermal Engineering 30 (4) (2010) 376–383.

[17] Z. Mei, J. Mi, F. Wang, C. Zheng, Dimensions of ch4-jet flame in hot o2/co2 coflow, Energy & Fuels 26 (6) (2012) 3257–3266.

[18] Y. Kang, X. Lu, Q. Wang, X. Ji, S. Miao, J. Xu, G. Luo, H. Liu, Experimental and modeling study on the flame structure and reaction zone size of dimethyl ether/air premixed flame in an industrial boiler furnace, Energy & Fuels 27 (11) (2013) 7054–7066.

[19] G. Krishnamoorthy, A new weighted-sum-of-gray-gases model for oxy-combustion scenarios, International Journal of Energy Research 37 (14) (2013) 1752–1763.

[20] R. Johansson, K. Andersson, B. Leckner, H. Thunman, Models for gaseous radiative heat transfer applied to oxy-fuel conditions in boilers, International Journal of Heat and Mass Transfer 53 (1) (2010) 220–230.

[21] H. Abdul-Sater, G. Krishnamoorthy, M. Ditaranto, Predicting radiative heat transfer in oxy-methane flame simulations: an examination of its sensitivities to chemistry and radiative property models, Journal of Combustion 2015.

[22] P. Nakod, G. Krishnamoorthy, M. Sami, S. Orsino, A comparative evaluation of gray and non-gray radiation modeling strategies in oxy-coal combustion simulations, Applied Thermal Engineering 54 (2) (2013) 422–432.

[23] Z. Wheaton, D. Stroh, G. Krishnamoorthy, M. Sami, S. Orsino, P. Nakod, A comparative study of gray and non-gray methods of computing gas absorption coefficients and its effect on the numerical predictions of oxy-fuel combustion, Industrial Combustion (2013) 1–14.

[24] ANSYS Inc., Canonsburg, PA, ANSYS FLUENT User's Guide, Version 15 (2014).

[25] M. D. Smooke (Ed.), Reduced kinetic mechanisms and asymptotic approximation for methane-air flames: a topical volume, Vol. 384 of Lecture Notes in Physics, Springer-Verlag, Berlin, 1991.

[26] J. Van Doormaal, G. Raithby, Enhancements of the simple method for predicting incompressible fluid flows, Numerical heat transfer 7 (2) (1984) 147–163.

[27] S. Patankar, Numerical heat transfer and fluid flow, CRC press, Washington, DC, 1980.

[28] B. Leonard, S. Mokhtari, Ultra-sharp nonoscillatory convection schemes for high-speed steady multidimensional flow, in: NASATM1-2568 (ICOMP-90-12), NASA Lewis Research Center, 1990.

[29] H. K. Kim, Y. Kim, S. M. Lee, K. Y. Ahn, Studies on combustion characteristics and flame length of turbulent oxy- fuel flames, Energy & fuels 21 (3) (2007) 1459–1467.